

Combined effects of satellite and ion detector geometries and potentials on the measurement of thermal ions. The Hyperboloid instrument on Interball.

M. Hamelin¹, M. Bouhram¹, N. Dubouloz^{1,2°}, M. Malingre¹, S. A. Grigoriev³ and L.V. Zinin³

¹Centre d'Etude des Environnements Terrestre et Planétaires, 4, av. de Neptune, 94107 Saint Maurice, France
e-mail: michel.hamelin@cetp.ipsl.fr; tel.: 33 1 45114279; fax: 33 1 48894433

²Laboratoire de Physique et Chimie de l'Environnement, 45071 Orléans cedex, France

³Kaliningrad State University, Mathematical Dept., A. Nevski ul., 14, 236041 Kaliningrad, Russia

Abstract

The measurement of the full ion distribution on satellites is impossible if the detector potential meets a positive potential with respect to the ambient plasma. For that reason, and because satellites are often at positive potentials in the magnetosphere, caused by photoelectron emission, a negative bias can be applied on the Hyperboloid ion detector on the Interball-2 satellite as for the GEOS 1 & 2 and DE1 previous satellites. The aim of this work is to compute the perturbations of the ion distributions at the entrance of the detector and more generally to evaluate the real efficiency of the biasing technique. Most of the time the Interball-2 high altitude auroral satellite is charged at a few Volts positive potential with respect to the ambient plasma, as it can be deduced from electrostatic probes measurements. Then a bias, generally -8 V, is applied to Hyperboloid to set its potential negative, but obviously the lower part of the energy range 1-80 V of the instrument would be strongly disturbed. The ions reaching the Hyperboloid entrance windows would have travelled across a continuous huge electrostatic lens involving various spatial scales from ~ 10 cm (detector radius) to ~ 10 m (satellite antennas).

Neglecting space charge effects, we have computed 3D potential maps and then the ion trajectories able to reach the Hyperboloid windows within their acceptance angles. We show that, for given values of the satellite potential and for each direction of arrival (each window of the detector), there is an energy cutoff and that the efficiency of the biasing technique is poor because the instrument is very close to the spacecraft body. All ions with energy just above the cutoff can come from a large range of directions in the undisturbed plasma; so, for this particular energy range, the angular measurement becomes undetermined. For all upper energy ranges a precise angular correction can be applied to the measurements. Using an extremely simple two-spheres model, we finally discuss the improvements which could be used in further experiments in the absence or not of any active control of the satellite potential.

Introduction

The direct measurement of thermal plasmas from magnetospheric satellites or planetary probes is an extremely difficult task due to the perturbations caused by the presence of the spacecraft in the medium, especially for very low energies where the major part of the distribution is concentrated. An ideal thermal ion analyser should be polarized with a low negative potential with respect to the surrounding plasma in order to attract the lowest energy ions into the detector. In addition, satellite motion in the medium could either help or make more difficult the measurement of very low energy ions. Obviously, the polarisation should have been of opposite sign to detect electrons and the full distribution of both ions and electrons would never be accessible at the same time. Even the measurement of particle distributions of the same sign could necessitate several orientations and polarisation settings to determine the full distribution.

We will consider here the measurement of thermal ions with the Hyperboloid instrument on the Interball Auroral satellite. The analyser selects incoming ions against arrival directions through angular windows and against energy channels. For ions, the main difficulty arises when the satellite is in sunlight in a low density plasma where the satellite potential could rise a few volts positive or more (Pedersen, 1995). As for other satellites as GEOS 1 & 2 and DE1 (Decrau, 1978), the instrument potential can be biased relatively to the spacecraft in order to reduce the potential barrier around the satellite. An ion source was also used to artificially control the satellite potential but it failed during the early part of the mission. In practice, to analyse the Hyperboloid data in high altitude depleted plasmas, we have to face the problem raised by the photoelectron induced potential barrier. More complicated than a simple barrier, the ions have to pass through a complex 3D electrostatic optical system involving several space scales from the cm scale of the detector to the 10 m scale of the antennas deployed around the satellite. For a given potential of the satellite, measured by electric probes, we computed a detailed potential map around the satellite and then inverse trajectories starting from the detector windows. We deduced an angular correction for the direction of arrival of the ions which energies are some gap higher than the potential barrier. The complicated effect on the ions which energies are close to the potential barrier

is discussed on the basis of a statistical study. We show that the biasing technique as applied in the case of Interball-2 has a limited effect due to the location of Hyperboloid practically stuck on the satellite surface. Finally, on the basis of a very simple model, we discuss the possibilities to measure almost all the thermal ion distribution using the biasing technique but with the ion detector held by a relatively long boom.

The Hyperboloid ion analyzer on Interball-2

The Hyperboloid instrument (Dubouloz *et al.*, 1998) aboard the Interball-2 satellite is an ion mass spectrometer measuring three-dimensional distributions of low energy ions (<80 eV) at altitudes from 700 to 20000 km, over the auroral zone. The instrument has been designed to select the major ion species against mass and charge (H^+ , He^+ , O^+ and O^{++}), against several energy ranges and against their direction of arrival through the multiple windows of its two analysers taking also benefit of the rotation of the satellite (Dubouloz *et al.*, 1998). The Interball-2 configuration with solar panels and antennas is shown in Figure 1. The Hyperboloid main analyser A16 lies in a plane parallel to the spin axis as shown in Figure 2a, whereas Figure 2b shows the angular pointing directions of the 16 windows. The windows have acceptance angles of about $10_j \times 10_j$ (for details, see Dubouloz *et al.*, 1998).

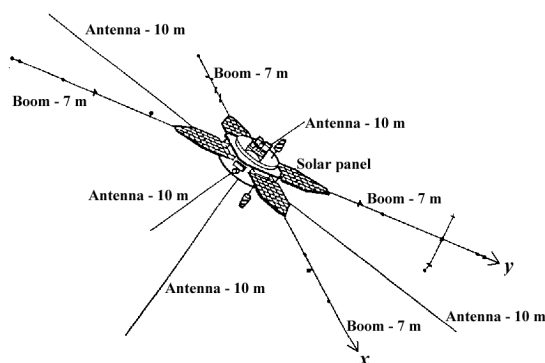


Figure 1. INTERBALL-2 satellite

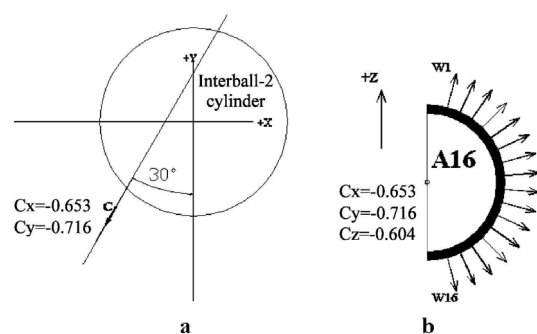


Figure 2. HYPERBOLOID ion analyser A16 (a: location of the analyser plane; b: directions of the windows)

Statistical observations from the IESP electric field double probe experiment (Perraut *et al.*, 1998) aboard Interball-2 have shown that the S/C body potential reaches positive values ranging from 0 to 12 V (Torkar *et al.*, 1999). Since the low-energy part of the measured ions is comparable to the typical S/C potentials, a precise knowledge of both S/C body potential and the three-dimensional potential distribution surrounding the body is required to correct the measured ion distributions. The simulations of the spacecraft-plasma interaction in Bouhram *et al.* (2001_b) led to the spacecraft potential in various conditions of plasma density and photoemission characteristics. For the low plasma densities as encountered on the Interball-2 orbit, it is shown that the space charge has a minor influence to the potential structure around the spacecraft. Then, we considered that the potential is the solution of the Laplace equation with the spacecraft at a potential inferred from IESP measurements and theoretical considerations (Bouhram *et al.*, 2001_a).

Potential maps and ion trajectories

The potential 3D map has been calculated as the assembly of 3 maps representing a large scale picture embedding the spacecraft with all antennas, a medium scale, and a small scale describing with a 2.5 cm grid the satellite, the solar panels and HYPERBOLOID (for details, see Zinin *et al.*, 1998; Hamelin *et al.*, 2001). The outer large scale grid size is $80 \times 80 \times 60$ m with 0.5 m spacing. At distances to the analyser closer than the grid spacing, the potential is estimated analytically owing to the cylindrical shape of the analyser. An interpolated map showing the potential in the analyser plane when the satellite potential $V_s = +4$ V and the analyser potential $V_h = -4$ V is shown in Fig. 3. It shows only a 1.3 meter square around the analyser (in white) with the middle of the spacecraft on the left. We see a saddle configuration with an absolute potential barrier level of ~ 2.3 V at the saddle point. Then, the efficiency of the biasing technique is ~ 1.5 V in the best case. Close to the top, the potential is near the spacecraft potential due to the influence of the solar panels. Looking at this figure, one can expect lower angular deviations for ions passing through the saddle configuration and incoming into HYPERBOLOID in windows 11-15 of Fig. 2b.

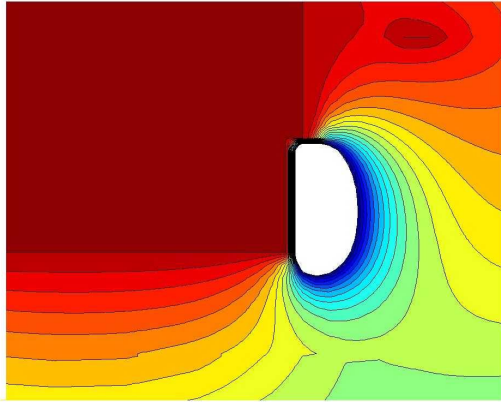


Figure 3. Potential map in the analyser plane [$V_s = +4$ V; $V_h = -4$ V; potential step: 0.2 V]

Single inverse ion trajectories in the computed electrostatic field were derived with a Runge Kutta integration scheme, starting from the individual Hyperboloid windows. The ions could: i) return into the detector, which means that these ions should be never observed, ii) hit the satellite body or any solar panel or antenna (then these items shadow the detector windows), iii) cross the external border of our computational domain, a 30 m radius sphere^o: the inverse trajectories can then be those of magnetospheric thermal ions detected by Hyperboloid. In the last case, the ions outgoing in the central direction of each window are deflected in the 3D potential structure leading to some angular deviations depending on the energy (and charge number). Difficulties occur for energies above but close to the cutoff; for a slight change of energy the ions can have completely different trajectories. A worse case example is given in Fig. 4, for another case where $V_s = 12$ V and $V_h = 4$ V. Ions incoming in the upper windows with an energy in the range (5-7 eV with respect to the analyser potential) can come either from the top right or from the bottom right of the figure. The ions starting from the window with energies lower than 5 eV return to the analyser, so they cannot be detected whereas ions with energies greater than 7 eV are slightly deviated closer to the pointing direction as the energy increases. The reflection of the 5-7 eV ions is explained by the solar panels influence; when an ion reaches the vicinity of a maximum of potential with a very small kinetic energy, the further direction becomes very unstable.

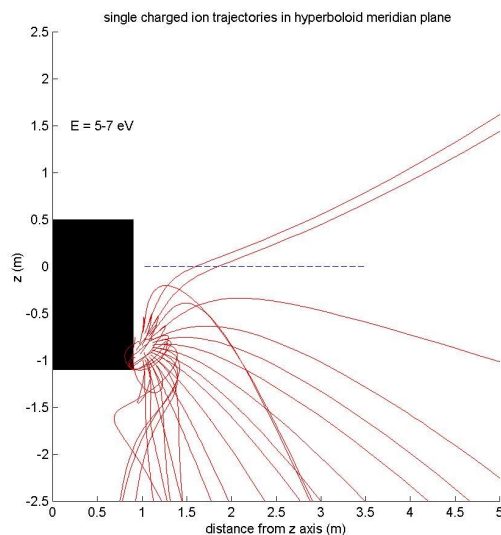


Figure 4. Projection of 3D ion trajectories on the A16 analyser plane for $V_s = 12$ V and $V_h = 4$ V (see text).

Incoming direction probabilities

The calculations of single trajectories is not sufficient to understand the measurements of the Hyperboloid analysers. In practice, the individual windows are selecting ion species in narrow energy channels and in about $10_i \times 10_i$ angular windows. Then the question is to determine from what original direction are coming the detected ions, knowing the energy shift through the estimated satellite potential and the potential bias. For that, we compute the incoming directions on a statistical basis, taking a large number of ions (4000 in practice) with random energies in the considered energy channel and random directions in the window angular widths. The computed directions at the end of the inverse trajectories, when the ion exits the 30 m sphere, are accumulated in (also) $10_i \times 10_i$ angular pixels on the sphere. With the example of $V_s = 4$ V and $V_h = -4$ V; the results are reported in Figure 5. The usual θ polar angle (from the z axis of Fig. 1) range is $(0-90_i)$ and the ϕ azimuth (from the x axis) range is $(90-360_i)$. The A16 analyser is pointing at $\phi = 240_i$. We do not present the lower five energy channels which are all below the cutoff and we do not present the upper eight channels for which there is a relatively small deviation and no spreading.

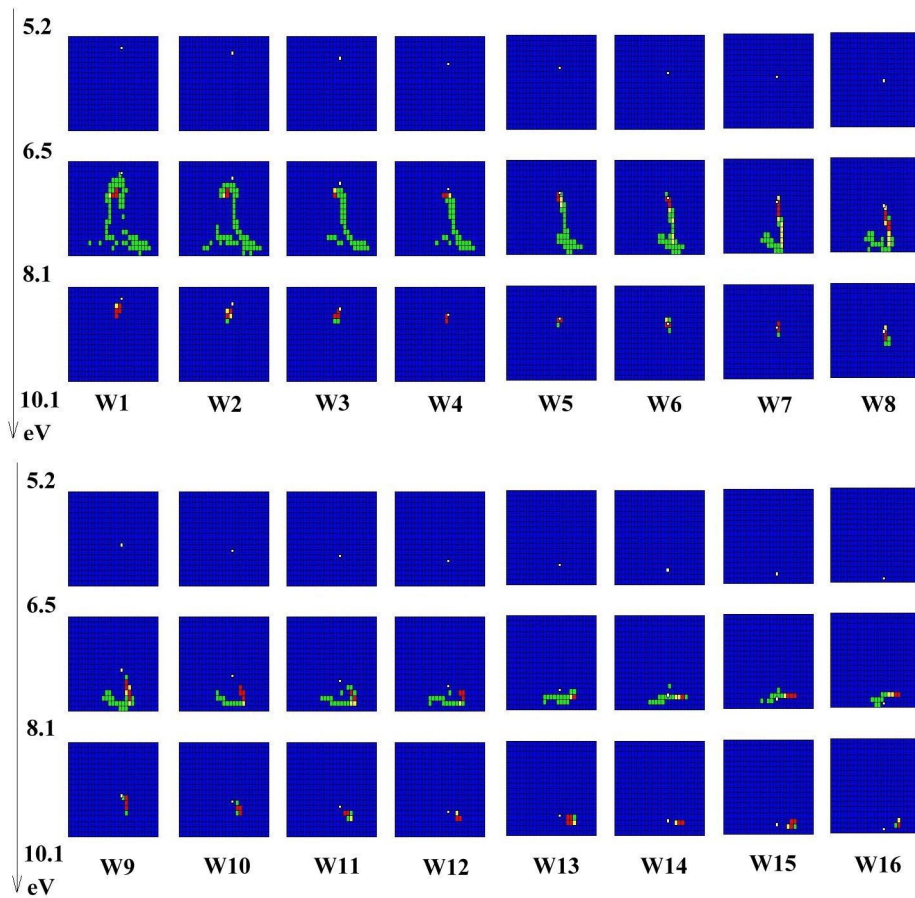


Figure 5. Probabilities of incoming direction for a particle detected by a window and within an energy gap. The horizontal axis display the polar angle (top: 0_i to bottom 180_i) and the azimuthal angle (left: 90_i to right: 360_i) respectively, with an angular resolution of 10_i . White squares indicate the geometrical viewing direction of each window. Colors indicate the probability level of each pixel: green for less than 3%; yellow for between 3% and 10%, and red for more than 10%.

The upper windows, (w1 to w8), for the first passing energy range of $[6.5-8.1$ eV], exhibit a remarkable dispersion^o at all angles close to the A16 plane, shifting to the left of the figures, and in a widely ϕ -spread structure around the direction which corresponds normally to lower windows. This effect can be understood as the ions which are passing at the top of a potential barrier are very slow here and can be easily deflected as we predicted; then, the solar panels potential structure acts as an electrostatic mirror. The figure looks asymmetric as the Hyperboloid environment is not symmetric, especially with the proximity of an antenna (POLRAD experiment antenna). In practice, the eight lower windows w9 —

w16 present a relatively low θ dispersion corresponding to a relatively free direction across the saddle potential structure of Fig.3. The wider azimuthal spreading is related to the lens effect caused by the adjacent long antennas (see Fig. 1).

The potential map of Fig. 3 shows the same saddle structure than on the potential maps computed by Olsen et al. (1986) around the DE1 satellite. The saddle point determines the absolute height of the potential barrier that the ions have to cross to reach the instrument. With our statistical calculation, we can derive a precise energy cutoff for each window. For the energy channel just above the cutoff, the probability maps exhibit a large dispersion of incoming directions probabilities. This is of little help for the experimenter as the natural ion fluxes are a priori anisotropic, so, we find out that we cannot measure the real incoming direction in this particular energy channel. For all other above energy channels precise corrections can be introduced in the data analysis software to provide the ion angular distributions.

The ion analyzer on a boom: an alternative to active potential control

In the case of HYPERBOLOID as for other similar instruments the lack of efficiency of the biasing technique is due to the close vicinity of the satellite body which, with its very large surface, governs the equilibrium of the system with the plasma. If the biased detector was at some large distance from the satellite body, the potential barrier would have been lower. In the following simple example, we model the satellite as a sphere of radius 1 m, the detector by another sphere of radius 10 cm. In the 3 examples with several distances from the detector to the satellite we set the satellite to +10 V and the detector to -10V (we use in fact in normalised dimensions). The colour step is 1 V (infinity value: 0 V).

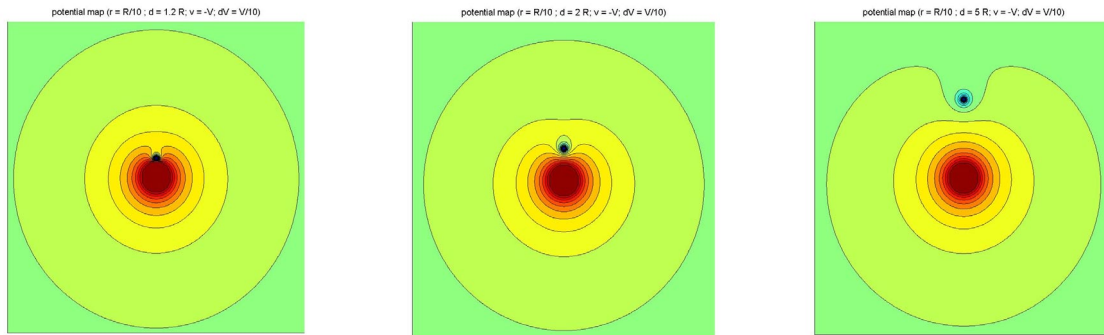


Figure 6. Potential between two conductive spheres for various distances (sphere radius: R and r for the satellite and the detector respectively; d: distance between centers; V and v: satellite and detector potentials; dV: contour step).

The first panel represents roughly the HYPERBOLOID case. The detector is “stuck” to the satellite and the potential barrier remains high. For the second case ($d = 2$ m), the potential barrier lies between 2 and 3 V. For the last case ($d = 5$ m), the potential barrier is smaller than 1 V. In any case, the detector should be aimed to the boom direction. Far from this optimal direction, the potential barrier could be a little more than 1 V and angular corrections should be necessary due to the deviation induced by the potential structure.

Now, increasing the bias to -60 V ($V_d = -50V$), we obtain the potential map of Figure 7. The potential barrier is then much less than 1V and the potential structure around the detector is smooth. The corrections to the incoming directions should be easily tractable in a 2π solid angle around the boom direction. However, the detector should have a relatively high energy resolution to discriminate small energy differences around 50 V.

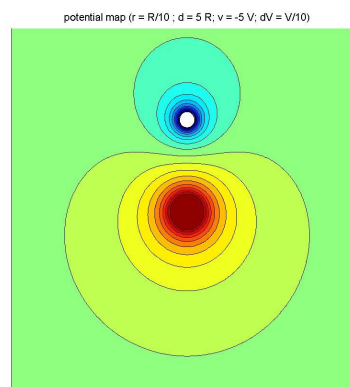


Figure 7. Same as figure 6, with $d = 5 R$ and $v = -5 V$

Conclusion

We have shown with the example of HYPERBOLOID that in the case of satellite positive charging, the measured ion distribution remains truncated even with the use of the biasing technique. Knowing the satellite potential, the measurements of the distribution of ions above some energy threshold can be corrected. A way to reduce this threshold would be to install the ion detector apart from the satellite body, held by a boom or a tether.

Generally, positive charging of the satellites is an intrinsic difficulty to measure the distributions of thermal ions. There are basically two ways to overcome the difficulty:

1) to control actively the potential of the satellite by ejection of energetic identified ions. In principle, it is possible to measure the full distribution of thermal ions. The practical difficulties are then the control of the potential to a given stable value and the induced perturbations of the surrounding plasma, including instabilities and waves.

2) to hold the analyser apart by a boom or a tether. The satellite remains at its equilibrium potential with the medium. The instrument which surface is only $\sim 1/100$ of the satellite surface is actively biased. The driving parameters are the ratio of the lowest measurable ion energy vs the maximum satellite potential and the length of the boom vs the satellite size. The impact on the medium is minimum. The full energy range is not covered but the lowest energy can be reduced according to the possible length of the boom.

Recent experience of active control of the satellite potential resulted in serious interferences with other instruments. The proposed alternative could be used in some favourable cases (3D stabilised or gravity gradient stabilized spacecraft or any other possibility to hold the detector apart from the satellite body). However, an active control of the satellite potential remains necessary to measure the really full ion distribution. A mix of the two techniques could reduce the impact of the potential control device which could also be used part of the time.

References

Bouhram, M., N. Dubouloz, M. Hamelin, S.A. Grigoriev, M. Malingre, K. Torkar, Y. Galperin, J. Hanasz, S. Perraut, R. Schreiber, and L.V. Zinin, Electrostatic interaction between Interball-2 and the ambient plasma. 1. Determination of the spacecraft potential from current calculations, submitted to *Ann. Geophys.*, 2001_a.

Bouhram, M., N. Dubouloz, and N. Singh, Sheath simulations for a high-altitude magnetospheric satellite^o: application to the Interball-2 case, submitted to *Geophys. Res. Lett.*, 2001_b.

Dcreau, P.M.E., J. Etcheto, K. Knott, A. Pedersen, G.L. Wrenn, and D.T. Young, Multi-experiment determination of plasma density and temperature, *Space Sci. Rev.*, **22**, 633-645, 1978.

Dubouloz, N., J.J. Berthelier, M. Malingre, L. Girard, Y. Galperin, J. Covinhes, D. Chugunin, M. Godefroy, G. Gogly, C. Gu rin, J.-M. Illiano, P. Kossa, F. Leblanc, F. Legoff, T. Mularchik, J. Paris, W. Stzepourginski, F. Vivat, and L. Zinin, Thermal ion measurements on board Interball Auroral Probe by the Hyperboloid experiment, *Ann. Geophys.*, **16**, 1070, 1998.

Hamelin, M., M. Bouhram, N. Dubouloz, M. Malingre, S.A. Grigoriev and L.V. Zinin, Electrostatic interaction between Interball-2 and the ambient plasma. 2. Influence on the low energy ion measurements with Hyperboloid, submitted to *Ann. Geophys.*, 2001.

Olsen, R.C., C.R. Chappell and J.L. Burch, Aperture plane potential control for thermal ion measurements, *J. Geophys. Res.*, **91**, 3117-3129, 1986.

Pedersen, A., Solar wind and magnetosphere plasma diagnostics by spacecraft electrostatic potential measurements, *Ann. Geophys.*, **13**, 118-129, 1995.

Perraut, S., A. Roux, F. Darrouzet, C. de Villedary, M. Mogilevski, and F. Lefevre, ULF wave measurements onboard the Interball auroral probe, *Ann. Geophys.*, **16**, 1105, 1998.

Torkar, K., H. Jeszenski, M.V. Veselov, S. Perrault, N. Dubouloz, C.P. Escoubet, and Yu.I. Galperin, Spacecraft potential measurements on board Interball-2 and derived plasma densities, *Cosmic Res.*, **37**, 606, 1999.

Zinin, L. V., Galperin, Y. I., Grigoriev, S. A. and T.M. Mulyarchik, On measurements of polarization jet effects in the outer plasmasphere, *Cosmic Research*, **36**, 42-52, 1998.